Learning for predictions: Real-time reliability assessment of aerospace systems

Learning for predictions: real-time reliability assessment of aerospace systems

Pier Carlo Berri*, Matteo D.L. Dalla Vedova† and Laura Mainini‡
Politecnico di Torino, Turin, Italy, 10129

Prognostics and Health Management (PHM) aim to predict the Remaining Useful Life (RUL) of a system and to allow a timely planning of replacement of components, limiting the need for corrective maintenance and the down time of equipment. A major challenge in system prognostics is the availability of accurate physics based representations of the grow rate of faults. Additionally, the analysis of data acquired during flight operations is traditionally time consuming and expensive. This work proposes a computational method to overcome these limitations through the dynamic adaptation of the state-space model of fault propagation to on-board observations of system's health. Our approach aims at enabling real-time assessment of systems health and reliability through fast predictions of the Remaining Useful Life that account for uncertainty. The strategy combines physics-based knowledge of the system damage propagation rate, machine learning and real-time measurements of the health status to obtain an accurate estimate of the RUL of aerospace systems. The RUL prediction algorithm relies on a dynamical estimator filter, which allows to deal with nonlinear systems affected by uncertainties with unknown distribution. The proposed method integrates a dynamical model of the fault propagation, accounting for the current and past measured health conditions, the past time history of the operating conditions (such as input command, load, temperature, etc.), and the expected future operating conditions. The model leverages the knowledge collected through the record of past fault measurements, and dynamically adapts the prediction of the damage propagation by learning from the observed time history. The original method is demonstrated for the RUL prediction of an electromechanical actuator for aircraft flight controls. We observe that the strategy allows to refine rapid predictions of the RUL in fractions of seconds by progressively learning from on-board acquisitions.

I. Introduction

Prognostics and Health Management (PHM) are key enablers for improving the safety and reducing the environmental impact of aircraft system operations. PHM relies on the prediction of the residual time before the failure of equipment, which is commonly referred to as the Remaining Useful Life (RUL) of components and systems. A widespread adoption of those techniques would result in a more efficient planning of maintenance actions, and a reduction of the required spares [1]. Most approaches to RUL prediction available in literature focus on offline execution during maintenance, and are only able to deal with failure modes that evolve slowly compared to the mission of the vehicle. In contrast, a PHM performed onboard, in nearly real-time, would ease the introduction of novel design solutions and the integration of novel technologies. The improvement in mission reliability offered by real-time prognostics would allow to consider innovative, although less consolidated, system configurations for flight applications, without compromising safety. Greener and more efficient design solutions, such as more-electric and all-electric system architectures could be employed safely and extensively [2, 3]. Eventually, real-time PHM would support a future relaxation of redundancy requirements, that are now necessary to guarantee safety.

With the PHM approach to system lifecycle management the Remaining Useful Life (RUL) of components is estimated dynamically, based on the current health status of the system. The real-time response is analyzed to detect the early signs of failure modes, and maintenance activity is planned in advance to perform the required preventive and corrective actions.

*PhD Candidate, Dept. of Mechanical and Aerospace Engineering, Politecnico di Torino, c.so Duca degli Abruzzi 24, Turin, 10129, IT, AIAA Student Member.

†Assistant Professor, Dept. of Mechanical and Aerospace Engineering, Politecnico di Torino, c.so Duca degli Abruzzi 24, Turin, 10129, IT

‡Adjunct Professor, Dept. of Mechanical and Aerospace Engineering, Politecnico di Torino, c.so Duca degli Abruzzi 24, Turin, 10129, IT, AIAA Associate Fellow

The RUL estimate is unavoidably affected by uncertainty associated with a variety of elements. First, the detection of the current health status (Fault Detection & Identification) can be affected by measurement errors due to the accuracy of the acquisition technologies, the disturbance caused by the variability of operating conditions, or the uncertainty associated with modelling the behavior of the faulty system. The uncertainty that affects the detection and identification of the faults propagates to the estimate of the remaining useful life, and might lead to a potentially large error in predicting the reliability properties of the system [4, 5]. In addition, the complexity of aircraft systems causes multiple failure modes to potentially interact in a manner that is difficult to predict analytically: hence, models of damage propagation rate are commonly affected by significant structured and unstructured uncertainties [6, 7]. Finally, the mission profile of the system, that is the operating and environmental conditions, is inherently unpredictable: this particularly holds when dealing with equipment intended for aircraft (or in general vehicle) applications, as opposed to industrial systems which commonly operate in a more controlled environment [8].

The investigation and development of methods for the rapid estimate of the remaining useful life as a measure of system's reliability is gaining a lot of interest in the engineering community, since a reliable, real-time RUL prediction could bring huge benefits in terms of maintenance costs related to the operation of a fleet of vehicles. Okoh et al. [9] provide a review of methods for the prediction of Remaining Useful Life of systems. Karandikar et al. [10] discusses the use of Bayesian Inference for the estimation of RUL of tools for machining processes; this method requires large experimental datasets and is difficult to exend to multiple failure modes. Grosso et al. [11] compare the performance of Long-Short Term Memory (LSTM) neural networks and Particle Filtering for prognostics of industrial automation equipment: while the former tends to be less precise on long term predictions, the latter requires computational efforts not suitable for real-time evaluations. Additionally, most of these approaches deal with industrial equipment, intended to operate in a semi-controlled environment and with a repeatable operation sequence.

We propose a strategy to obtain a nearly real-time estimate of the Remaining Useful Life of a dynamical system by acquiring and processing its response. We combine an adaptive physics-based knowledge of the damage propagation rate with surrogate modeling of the system performance to obtain an accurate and computationally efficient estimate of the RUL of the equipment, which in turn gives a measure of the current reliability of the system. Specifically, we introduce an original algorithm for the real time estimate of the remaining useful life of aerospace systems which leverages a dynamical estimator filter [12, 13] that runs in parallel with a system identification routine and corrects the instantaneous estimate of the health condition with predictions given by a model.

This approach permits to deal in a computationally efficient manner with the two issues usually associated with the RUL estimation. On one hand, the dynamical estimator filter allows to deal with the uncertainties associated with the FDI: the RUL estimation accounts for the entire observed health time-history and compares it to a reference model to discriminate between random FDI errors and the actual health evolution, instead of considering uniquely the last detected health condition. On the other hand, the system identification routine deals with the uncertainty associated with the model of damage propagation. The initial model is progressively updated and calibrated in real-time to match the time-evolution of the health condition actually experienced by the equipment. This strategy also allows to account for unexpected variations in the environmental and operating conditions.

In addition, the proposed strategy is designed to obtain a major reduction of the computational time for the estimation of Remaining Useful Life that is suitable for real-time onboard computations. The computational burden is very low in comparison with similar approaches (such as those based on particle filtering [14]). Our method is assessed in combination with a hybrid physics-based and data-driven Fault Detection and Identification (FDI), originally introduced in [4]. This employs an optimal sampling technique to compress information received from installed sensors, and computes in nearly real-time an estimate of the current system health condition through projection-based model order reduction and supervised machine learning. The approach is demonstrated for the prognostic analysis of an electromechanical actuator for aircraft flight controls. The application over different fault case is discussed and quantitative results assessing accuracy and computational effort are proposed.

In this manuscript, Section II details the proposed PHM methodology, Section III describes a possible application to aircraft actuation systems and Section IV discusses the results of our investigation.

II. Methodology

A typical PHM process can be divided into three tasks: (1) Data Acquisition, (2) Fault Detection & Identification (FDI) and (3) RUL estimation. In the Data Acquisition task, the sensors installed on the system measure a set of working parameters, which are sampled at a given frequency and stored on a memory support. Ideally, these sensors are installed to guarantee the nominal operations of the system. For example, they are employed for closing feedback loops, or to

give indications to the pilot. This way, the PHM process leverages the data already available, and does not require the installation of additional hardware with the associated weight, cost, and failure rate.

In the FDI task, data are analyzed to uncover the underlying characteristic features of physical fault modes. For example, a partial short circuit of an electric motor may cause an increase in current to produce a given torque, or the wear of a bearing can result in vibrations at a specific frequency. Several algorithms can be used, either model-based [15, 16], data-driven [17, 18] or combinations of both [19, 20]. Model based FDI relies on the comparison of the measured dynamical behavior of the system with that of numerical simulations, able to determine the effect of faults. For example, Sidhu et al. [21] propose to employ the residual between the actual terminal voltage and that estimated by a Kalman Filter to detect fault signatures in lithium batteries. Kim and Parlos [22] employ multiresolution signal processing methods to diagnose faults of induction motors. Data driven FDI leverages machine-learning algorithms trained on a dataset, gathered from an experimental campaign and representative of the common failure modes affecting a given system. In [23], Qin proposes the use of multivariate statistics tools to monitor complex industrial processes. Sarkar et al. [24] leverages symbolic dynamic filtering to estimate the health condition of aircraft gas turbines accounting for sensor noise.

The RUL estimation task exploits the information on the current health status of the equipment to compute its Remaining Useful Life. This is usually done both by analyzing the damage propagation rate and by leveraging models of the degradation of components. The first phase is necessarily performed in real-time; the others are usually executed offline since they involve a high computational cost.

Our goal is to develop suitable algorithms to accurately and reliably achieve RUL estimation in real-time in order to enable a continuous monitoring of the aircraft critical systems, such as the flight control actuators. This would not only result in increased safety of the operations, but also in the possibility to adapt in-flight the mission profile and system control laws in order to deal with an off-nominal condition. We propose a novel RUL prediction process that learns in real-time a model for the fault growth rate from the available observations, and accounts for the uncertainties associated with the previous Fault Detection and Identification task. The algorithm is tested in combination with the compression and FDI strategies proposed in the PHM framework discussed in [5]. The framework covers the three main PHM tasks of signal acquisition (Section II.A), FDI (Section II.B) and RUL estimation (Section II.C): model-based and data-driven approaches are combined to reduce the computational burden associated with each phase and to enable real-time fault detection and RUL estimation. Each of the three PHM tasks is split into two phases: an offline training and an online evaluation. Offline we learn efficient models from data and physics, online we use those models to obtain rapid predictions of the remaining useful life from acquired physical signals. The entire prognostic computational framework employed in this work is represented schematically in Figure 1.

A. Signal Acquisition and Compression

We address the signal acquisition and compression phase to reduce the amount of data to store and process, while retaining the useful information about the health condition of the monitored system. To this purpose, offline we determine a set of informative time locations in which the output of the system will be measured and analyzed online.

1. Offline

A training set of n_s output signals of the monitored system is collected, either from experiments, historical records of field data, or simulations: the latter approach is employed in this work. Each signal from the dataset is associated with a different combination of faults affecting the system, and the output of the system shall be chosen so that it is sensitive to the considered fault modes. The output signals are arranged into the columns of a measurement matrix Y, and the principal components $\boldsymbol{\nu}$ of the dataset are computed through Proper Orthogonal Decomposition (POD) [25, 26]. POD is a procedure commonly employed for model reduction that processes possibly correlated data searching for underlying structures. Candes et al. [27] employ POD for robust signal recovery in presence of measurement uncertainty; in [28], POD is leveraged to solve optimal control problems for closed-loop control.

POD allows expressing each signal $\boldsymbol{y}$ of the training dataset in the form:

$$\boldsymbol{y} = \boldsymbol{y}_0 + \sum_{i=1}^{n_s} \boldsymbol{\nu}_i \boldsymbol{\alpha}_i \tag{1}$$

where $\boldsymbol{y}_0$ is a baseline signal and $\boldsymbol{\alpha}_i$ are the POD coefficients. By truncating the expansion to the first $n_m \ll n_s$ modes, a reduced representation of the signal is obtained.

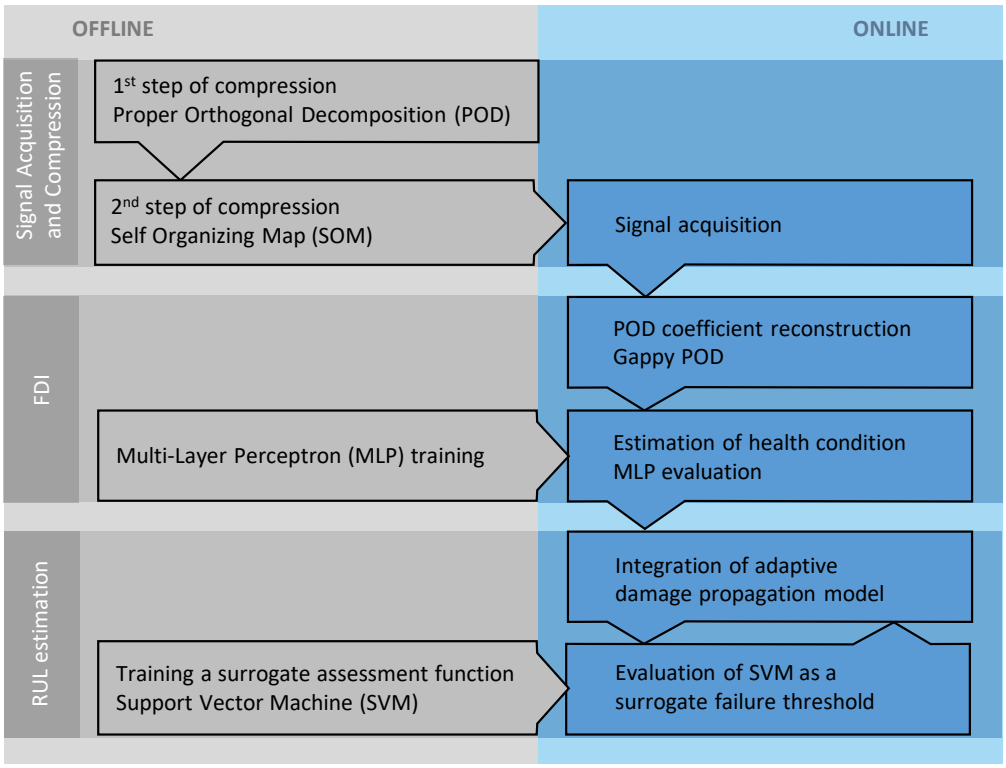

Fig. 1 Overview of the PHM framework employed in this work

A second step of compression leverages the properties of Self Organizing Maps (SOM) to obtain an compression mask in form of a set of informative time locations for the signal $\boldsymbol{y}$. SOMs are a class of single layer neural networks employing unsupervised learning to find clusters of self-similar points in a training dataset [29]. In [30], SOMs are employed as a classifier for diagnosing failure modes of induction motors. Svensson et al. [31] propose the use of SOMs enabling automatic fault detection of a fleet of vehicles.

In this paper, an SOM is trained with a dataset $T = [\boldsymbol{t}^\top \boldsymbol{v}_1^\top ... \boldsymbol{v}_{n_m}^\top]$, including the first n_m components of the signal $\boldsymbol{v}_i$ and the associated time-coordinates $\boldsymbol{t}$. After training, the components of the weight vectors of the SOM associated with the time input encode a set of informative time-locations to be employed online to measure the system output. The approach, introduced in [32, 33] for structural applications, was applied to fault detection of dynamical assemblies with promising results [4, 5].

2. Online

The signal is measured and stored only at the informative time locations determined offline, to obtain the compressed measurement $\hat{y}$. Then, Gappy Proper Orthogonal Decomposition (Gappy POD, [34]) is exploited to estimate the POD coefficients associated with the newly measured signal. Specifically, an estimate of the coefficients $\boldsymbol{\alpha}$ is obtained by solving the linear system:

$$\mathrm{G}\boldsymbol{\alpha} = \boldsymbol{f} \tag{2}$$

where $\mathrm{G} = \hat{\mathrm{v}}^\top \hat{\mathrm{v}}$ is the gappy matrix, $f = \hat{\mathrm{v}}^\top \hat{y}$ is the projection of the compressed measurement $\hat{y}$ along the compressed POD modes $\hat{\mathrm{v}}$. Those coefficients encode a compressed representation of the signal, more robust to noise and uncertainty than the direct signal measurement, to be employed for FDI.

B. Fault Detection and Identification

Fault Detection and Identification (FDI) leverages supervised machine learning to create a map from the POD coefficients to the fault condition. Specifically, a Multi-Layer Perceptron (MLP) [35] is trained offline and evaluated online in order to determine the faults affecting the system.

1. Offline

The training set is assembled with the POD coefficients associated with the n_s signals of the initial dataset, and the fault combinations employed to compute each signal. A standard MLP formulation is adopted, including a single hidden layer with sigmoid activation function and an output layer with linear saturated activation function. MLPs are Artificial Neural Networks relying on supervised learning to obtain computationally efficient models for data regression or classification. The particular choice of the activation functions is motivated by the specific characteristics of the considered problem: the linear saturated output layer permits to produce a bounded health condition estimate; differently than a continuous sigmoid function, the output tends to stick to the lower bound (i.e. a completely healthy system) when the system behavior is nearly nominal, limiting the risk of false positive FDIs. The choice of this particular network layout and topology is discussed in Berri et al. [5], which demonstrated the effectiveness of this particular MLP configuration in providing estimates of fault states from reduced and compressed current signals. The MLP model is trained through a Levenberg-Marquardt backpropagation algorithm [36, 37].

2. Online

The MLP model trained offline maps the POD coefficients $\boldsymbol{\alpha}_i$ into the fault condition $\boldsymbol{k}$. The model is evaluated online to compute the fault condition from the POD coefficients reconstructed via Gappy POD (Section II.A.2).

C. Estimation of Remaining Useful Life

The last phase of the PHM process is the actual estimation of the Remaining Useful Life. The input for the process is the current health condition determined by FDI, employed as a starting point for the evaluation of a model of damage propagation. The Remaining Useful Life can be formally defined as the remaining time before a performance parameter of the system hits a failure threshold:

$$\begin{aligned} &\text{RUL} = \max(t) \\ &\text{s.t.} \quad \phi_a(\boldsymbol{k}(t)) = \text{“healthy”} \end{aligned} \tag{3}$$

where $\phi_a(\boldsymbol{k}(t))$ is a function for the assessment of the system health, that evaluates the system performance under the health condition $\boldsymbol{k}$ and compares it to any applicable requirements.

The approach discussed in this work is inspired by structural health monitoring strategies associated with the damage tolerant design paradigms that are adopted for material fatigue [38]. In the field of structural health monitoring, the components are inspected periodically in search of cracks. Since the rate of propagation of cracks in metal and composite structure is known and well described by physics based models, the next inspection is planned before the existing cracks reach a critical length; if no cracks are detected during the inspection, they are assumed to be just below the sensitivity of the employed equipment.

The extension of this approach to systems poses two issues. First, the higher complexity of the monitored equipment makes accurate inspections impractical in periodical maintenance; then, this study proposes to replace, at least in part, manual inspections with the automatic, real-time FDI process described in Section II.B. Second, the heterogeneous disciplines that rule the propagation of faults results in the difficulty (or often in the impossibility) to determine an accurate physics-based model for damage propagation. To address this difficulty, we use an adaptive model for damage propagation, which is updated in real-time according to the observed time-history of the health condition.

Based on the definition of Remaining Useful Life of Equation 3, we employ a model of damage propagation in the form of a state-space dynamical model. The model is integrated numerically, starting from the combination of faults determined by FDI as the initial condition, and accounting for the entire observed time history of faults through a dynamic estimator filter. The simulation is adaptive and leverages a system identification algorithm to tune itself to match the observations. The function for the assessment of health condition is employed as a stopping criterion for the integration. This way, a failure threshold is set on the actual performance of the equipment, rather then on the fault parameters. This strategy permits to deal with combinations of multiple fault modes according to the definition of Remaining Useful Life as the remaining time after which the equipment will no longer meet the required performances:

when the estimated health condition reaches a value that is no more compatible with the requirements of the system, the corresponding integration timestep is assumed as the RUL estimate. The function for the assessment of the health condition requires the evaluation of a physics-based model to determine the performance of the faulty system. Therefore, computing the assessment function ϕ_a of Equation 3 is too expensive for time-constrained on-board computations. To enable real-time evaluation, a Support Vector Machine (SVM) is trained offline as a surrogate assessment function.

1. Offline

The function for health condition assessment $\phi_a(\boldsymbol{k})$ behaves as a binary classifier: it simulates the response of the system under the effect of the fault combination $\boldsymbol{k}$ and determines whether or not the applicable performance requirements are met by the equipment, assigning to $\boldsymbol{k}$ a binary output in the form of a "healthy" or "faulty" label. For simple application (like health monitoring of bearings, gears or other individual components, for which a low number of possible fault modes exist), the direct comparison of the fault vector with a threshold may be enough to determine the acceptability of a given health condition. However, this is usually not acceptable to deal with the combined effects of multiple fault modes affecting the equipment at the same time. More complex assessment functions quickly become impractical to evaluate in real-time. For example, a viable option for the health assessment of an actuator is to evaluate its transfer function with an iterative simulation at variable frequency of the command: this results in computational times of several seconds or more.

To enable real-time evaluation of the assessment function, this study proposes to employ a surrogate function in the form of a Support Vector Machine (SVM). SVMs are algorithms that leverage supervised machine learning to perform an efficient classification of the input data [39, 40]. In [41], SVM classifiers are employed to generate explicit decision functions for design optimization problems. Leng et al. [42] propose to combine SVMs and decision trees to improve computational time on large nonlinear problems.

To train a surrogate assessment function, we assemble a training set with the matrices $\mathrm{K} = [\boldsymbol{k}_1^\top, ..., \boldsymbol{k}_{n_s}^\top]^\top$ and $\Phi = [\phi_1, ..., \phi_{n_s}]$ discussed in Section 2.1. In the standard linear formulation, given a set of training points $\boldsymbol{k}_i$, each defined in $\mathbb{R}^{n_s}$, and their classes $\phi_i = \pm 1$, the SVM seeks an optimal hyperplane in $\mathbb{R}^{n_k}$ to separate the two classes. The equation of a generic hyperplane in $\mathbb{R}^{n_k}$ is:

$$f(\boldsymbol{k}) = \boldsymbol{k}^\top \boldsymbol{\beta} + b = 0 \tag{4}$$

where $f(\boldsymbol{k})$ is a cost function, $\boldsymbol{\beta}$ has the same dimensionality as $\boldsymbol{k}$ and b is a scalar bias. The goal of the training process for the SVM is to find the best separating hyperplane, that is, the one that results in the largest margin between the two classes $\phi = \pm 1$.

The training process employs the method of Lagrange Multipliers to find the optimal values for $\boldsymbol{\beta}$ and b, that maximize the margin between the two classes (or minimizes the classification error, if the training set is not linearly separable). After training, the function $\phi_a(\boldsymbol{k}) = sign(f(\boldsymbol{k}))$ is the surrogate function for the assessment of the health condition $\boldsymbol{k}$, to be employed in the online RUL estimation procedure.

2. Online

Remaining Useful Life is estimated online by integrating a model of damage propagation in form of a state-space dynamical model, which expresses the evolution in time of the health condition of the system, employing the surrogate assessment function $\phi_a(\boldsymbol{k})$ as a stopping criterion. A flow chart of the online procedure is provided in Figure 2.

The integration starts at time $t_0 = 0$, corresponding to the oldest known health condition $\boldsymbol{k}_0$ measured by the first FDI. The integration from t_0 to the current time t_{now} (that is, the time coordinate associated to the last FDI) accounts for the known time history of the fault vector $\boldsymbol{k}(t)$ in order to filter out uncertainties in fault detection and tune the model of damage propagation. Indeed, one of the most important challenges in system prognostics is that accurate physics-based descriptions of the fault growth rate are not commonly available. The proposed approach addresses this limitation by dynamically adapting a state space model to the real-time observations of the system's health. The general formulation of a state-space model is:

$$\begin{cases} \dot{\boldsymbol{k}} = \mathrm{A}\boldsymbol{k} + \mathrm{B}\boldsymbol{u} \\ \boldsymbol{j} = \mathrm{C}\boldsymbol{k} + \mathrm{D}\boldsymbol{u} \end{cases} \tag{5}$$

where A is the state matrix, B is the control matrix, C is the output matrix, D is the feedthrough matrix, $\boldsymbol{k}$ is the state, $\boldsymbol{j}$ is the observation, and $\boldsymbol{u}$ is the input. For the application to RUL estimate addressed in this study, we can

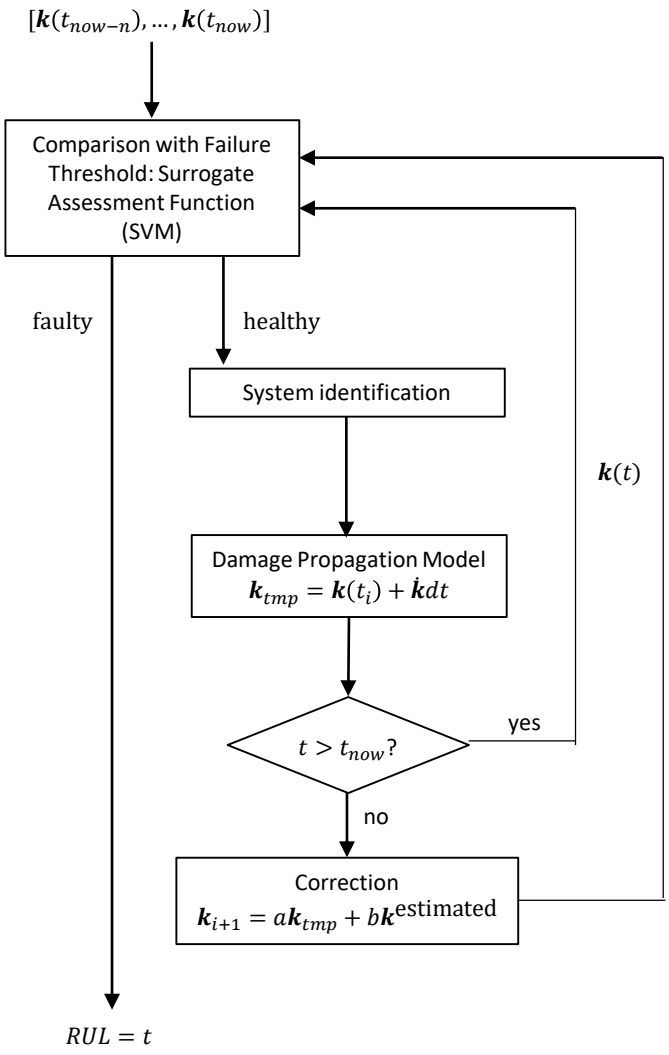

Fig. 2 Flow chart of the real-time procedure for RUL estimation

set $\boldsymbol{k} = [k_1 \ldots k_{n_k}]^\top$ as the health condition of the system, and $\boldsymbol{u} = [u_1 \ldots u_{n_u}]^\top$ as the environmental and operating conditions; the observation $\boldsymbol{j}$ can be considered equal to the state $\boldsymbol{k}$ (that is, the system health condition): then, we can neglect the second equation.

The state and control matrices may be derived from physics-based knowledge of the system. However, in this case a large uncertainty is usually associated with the state-space model, as the complex interactions between fault modes are difficult to derive from physical models and may be affected by unexpected changes in the operating conditions. Therefore, the matrices shall be estimated from observed data, allowing a more precise prediction of the evolution of faults. The elements of A and B can be computed from the equation:

$$\kappa_i a_i = \dot{\kappa}_i \qquad \text{for} \quad i = 1 \ldots n_k \tag{6}$$

where κ is a matrix containing the observed states $\boldsymbol{k}$ and inputs $\boldsymbol{u}$ of the last n timesteps:

$$\kappa_i = \begin{bmatrix} k_1(t_{now-n})) & \ldots & k_{n_k}(t_{now-n}) & u_1(t_{now-n}) & \ldots & u_{n_u}(t_{now-n}) \\ \vdots & \ddots & \vdots & \vdots & \ddots & \vdots \\ k_1(t_(now)) & \ldots & k_{n_k}(t_(now)) & u_1(t_(now)) & \ldots & u_{n_u}(t_(now)) \end{bmatrix} \tag{7}$$

a_i is a column vector with the elements of the i-th row of A and the i-th row of B:

$$a_i = [A_{i,1}, ..., A_{i,n_k}, B_{i,1}, ..., B_{i,n_u}]^\top \tag{8}$$

and $\dot{\kappa}_i$ is a column vector containing the time history of the i-th element of the state derivative $\dot{\boldsymbol{k}}$:

$$\dot{\kappa}_i = [k_i(t_{now-n}), ..., k_i(t_{now})]^\top \tag{9}$$

At each integration timestep, the matrices A and B are computed by solving the linear systems of Equation 6. The number of timesteps n is determined as a trade off between the need to filter out the uncertainties components from the observations (i.e. the errors of the FDI process), and the need to meet the time constraints imposed by the on-board computations. In any case, n shall be larger than $n_k + n_u$, i.e. the sum of the number of elements of the state and control vectors to guarantee that the system is not under determined; a number of timesteps larger than $n_k + n_u$ is allowed since Equation 6 can be solved in the least squares sense.

After the state and control matrices A and B are identified, the state-space model is employed for two purposes: as a dynamical estimator filter for the computation of the next fault condition, and as a predictor to extrapolate the future time evolution of the fault condition to determine the system RUL. The fault condition at the next timestep is estimated by fusing the information from FDI and the state-space system; this operates as a dynamical observer to filter the observations supplied by FDI. The method is similar to Kalman filtering, but does not make assumptions about the variance of the observations. The state is updated as a weighted sum of the prediction of the state-space model and the observation of the FDI procedure:

$$k_{i+1} = \gamma \boldsymbol{k}^e(t_{i+1}) + (1-\gamma)[\boldsymbol{k}_i + (\mathrm{A}_i \boldsymbol{k}_i + \mathrm{B}_i \boldsymbol{u}_i)\Delta t] \tag{10}$$

where $\gamma \in (0, 1)$ is a scalar weight parameter, $\boldsymbol{k}^e(t_{i+1})$ is the fault condition measured by the FDI procedure according to Section 2.3, and the term $\boldsymbol{k}_i + (\mathrm{A}_i \boldsymbol{k}_i + \mathrm{B}_i \boldsymbol{u}_i)\Delta t = \boldsymbol{k}_i + \dot{\boldsymbol{k}}_i \Delta t$ is the fault condition predicted by the integration of the model. This procedure can be used when the observations $\boldsymbol{k}^e$ are available, that is, for $t \leq t_{now}$. Since future fault condition are not measurable, the propagation of the state for $t > t_{now}$ is embedded by the state space model alone:

$$\boldsymbol{k}_{i+1} = \boldsymbol{k}_i + (\mathrm{A}_i \boldsymbol{k}_i + \mathrm{B}_i \boldsymbol{u}_i)\Delta t \tag{11}$$

At each time step t_i of the numerical integration, the surrogate assessment function $\phi_a(\boldsymbol{k})$ trained offline determines whether the equipment is still able to operate under the effect of the fault combination $\boldsymbol{k}(t_i)$. When a "faulty" condition is detected by the assessment function at time t_f, the integration is stopped, and the difference between the failure time and the current time is assumed as the RUL estimate:

$$\mathrm{RUL} = t_f - t_{now} \tag{12}$$

The proposed methodology permits to achieve a good accuracy in RUL prediction, even if the rate of propagation of the damage from its incipient state at t_0 to the actual failure at t_f is not known. This is often the case for complex mechatronic systems, where heterogeneous components described by different disciplines coexist and work together, sometimes interacting in ways that are difficult to predict analytically. Additionally, this method has a lower computational cost than comparable approaches available in literature (e.g. those based on particle filtering [43]) and can be executed in real-time on limited hardware resources.

III. Application

The proposed methodology is applied to prognostics and reliability assessment of aircraft Electro Mechanical Actuators (EMAs). These flight critical systems combine heterogeneous components which behavior is modeled by different branches of physics and engineering: electrical machines, electronics and software, rational mechanics, tribology, thermodynamics and heat transfer, fluid dynamics. As a result, the possible failure modes affecting such equipment are diverse; additionally, the contemporary presence of multiple failure modes results in effects that are different from the linear superposition of the individual faults. Then, the PHM task for this kind of systems is inherently challenging and constitutes a representative test case for the proposed methodology.

A. Dynamical model of the actuator

The EMA model considered in this paper is schematically represented in the block diagram of Figure 3. It is a lumped parameter model, which can be used in two different configurations: (1) for EMAs based on Brushless DC (BLDC) motors [44], and (2) for Permanent Magnet Synchronous Motors (PMSMs) [45]. This virtual representation of the electromechanical actuator is a multi-domain model and comprises electrical, mechanical and control components, which together simulate the multidisciplinary assembly of the physical actuator. The model can be described through the following five building blocks.

Actuator Control Electronics The Actuator Control Electronics (ACE) block emulates the PID control law that compares the position setpoint with the actual user position and speed, to compute a torque setpoint for the motor. The controller is able to switch between a position control mode and a speed control mode, and accounts for signal noise and digitization.

Actuator Power Electronics The Actuator Power Electronics block models the behavior of the three phase inverter that applies the required voltages to the motor coils, while controlling in closed loop the current and managing the phase commutation sequence.

Motor Electromagnetic Model The Motor Electromagnetic model computes the motor torque and current as a function of voltage and speed, by evaluating the electromagnetic coupling between the rotor poles and the stator windings. The model is able to account for the effect of multiple fault modes of the motor, including partial short circuit of the stator and eccentricity of the rotor shaft.

Motor-transmission Dynamical Model The Motor-transmission Dynamical Model is a nonlinear second order model for the motor and gearbox of the actuator. It accounts for viscous and dry friction between mechanical components, transmission backlash, endstops, and finite stiffness of the gears.

Load Model The Load Model is a simplified representation of the aerodynamic hinge moment acting on the actuator, assuming that it is employed for aircraft primary flight controls. It leverages the linearized longitudinal model of the F-16 fighter jet, available from Stevens [46] to evaluate the coupling between the dynamics of the actuator and aircraft.

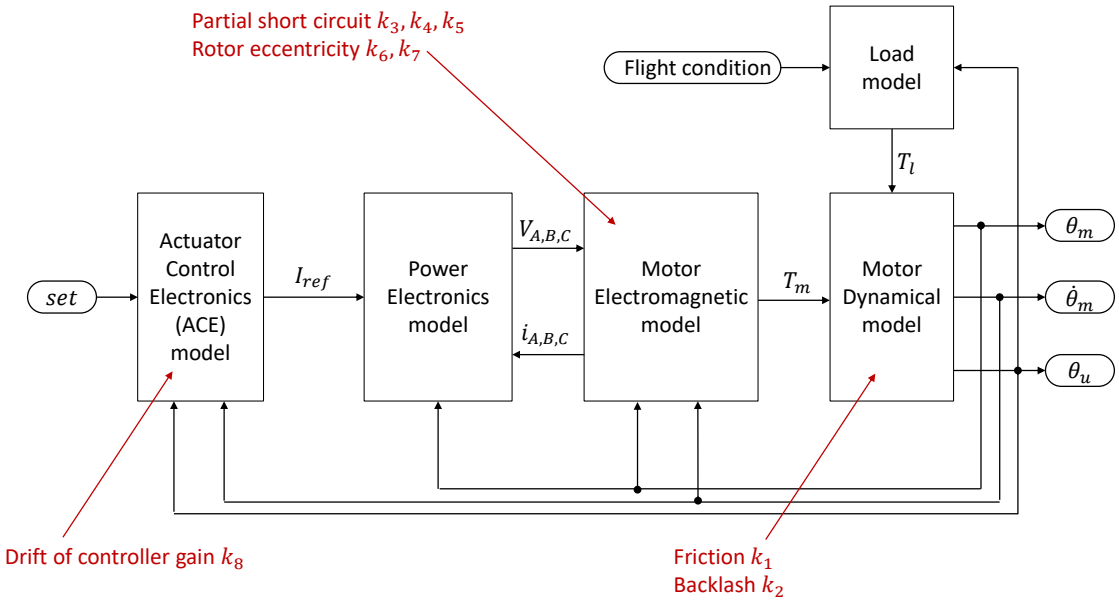

Fig. 3 Block diagram of the dynamical model of the actuator considered as a case study in this paper; the blocks affected by each fault mode is indicated in red.

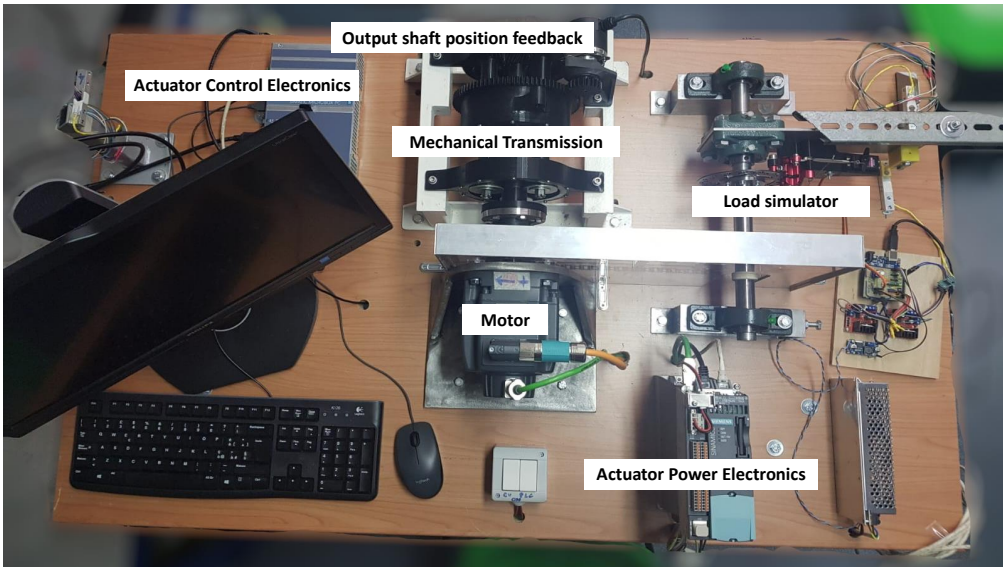

Fig. 4 Test bench employed for the validation of the EMA dynamical model

This EMA model allows to achieve high accuracy in predicting the behavior of the system in nominal and faulty conditions and has been validated against experimental data [47, 48]. Figure 4 illustrates the test bench employed to validate the output of the model in nominal conditions; the validation in presence of faults is currently in progress. The effects of 5 different fault modes are considered, namely friction (k_1) and backlash (k_2) of the mechanical transmission, partial short circuit (k_3 to k_5) and static eccentricity (k_6 and k_7) of the motor, and drift of the position control loop gain (k_8). The short circuit fault has three degrees of freedom, since it may affect each of the three electrical phases; the eccentricity fault depends on two parameters that encode the eccentricity measured in the two main directions perpendicular to the axis of rotation of the motor. As a result, the dimensionality of the fault vector $\boldsymbol{k}$ is 8.

The blocks affected by each fault mode are indicated in red in Figure 3. The signal monitored for prognostic purposes is the envelope of the three phase currents of the motor, as this quantity showed a good sensitivity to a variety of failure modes [4, 5]. The model is employed to compute high-fidelity reference data to train the data acquisition and compression (Section II.A.1) and FDI (Section II.B.1) algorithms. This virtual model, although much faster than a distributed parameter simulation, is about two orders of magnitude slower than what required for real-time evaluations: each second of simulated time requires about one minute of computational time on a common laptop PC.

B. Damage propagation model

The model of damage propagation adopted in this work is in the form of a state-space representation, where the damage propagation rate is a combination of two contributions: one is a function of the actual health condition and operating environment; the other is a normally distributed uncertainty, intended to account for the random fluctuations of operating conditions and the variability of characteristics and manufacturing defects of individual components. Those two contributions are captured in the state-space model as follows:

$$\dot{\boldsymbol{k}} = \mathrm{A}(t)\boldsymbol{k} + \mathrm{B}\boldsymbol{u} + \mathcal{N}(0, \sigma) \tag{13}$$

where $\mathrm{A}(t)$ is a piece-wise constant function whose changes happen randomly in time, and $\mathcal{N}(0, \sigma)$ is an independent and identically distributed noise affecting the damage rate $\dot{\boldsymbol{k}}$.

An example of fault propagation time history simulated by this model is shown in Figure 5. The vertical axis reports the components of the fault vector $\boldsymbol{k}$. Each component of $\boldsymbol{k}$ encodes the extent of one fault mode, either normalized with respect to its maximum allowed value. The black vertical line is the complete failure: a failure threshold is not represented as it is set on performance parameters, rather than on the individual fault parameters. For the specific example reported in Figure 5, the failure occurs at $t = 6700h$, when neither of the fault parameter alone exceeds its maximum allowable value, but the combined effect of all the fault modes results in unacceptable performances.

A variation in model parameters can be injected randomly during the simulation of the system operation. This

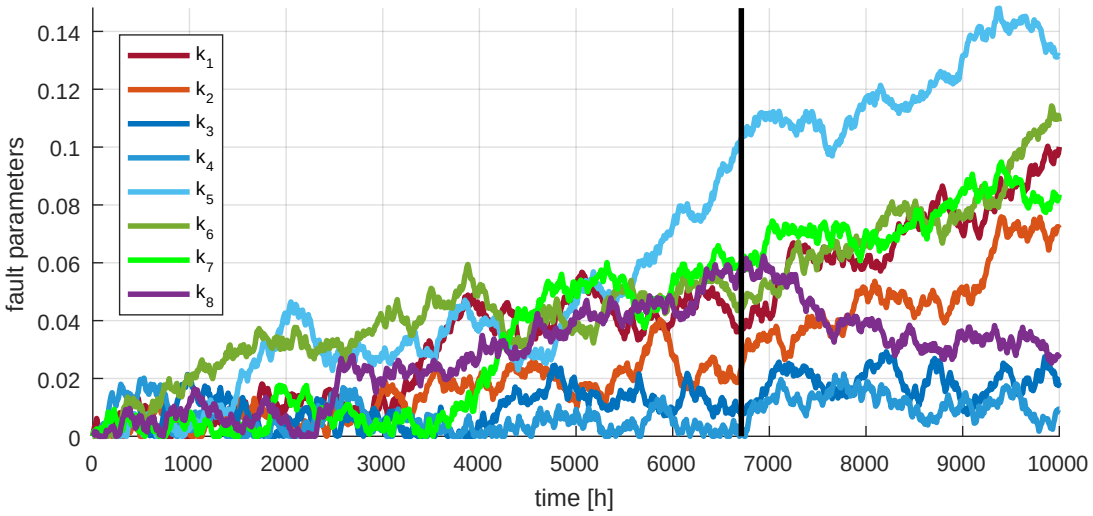

Fig. 5 Example of evolution of the system health condition. The black vertical line is the complete failure: the failure threshold is not represented as it is set on performance parameters, rather than on individual fault parameters

feature of the numerical model is used to simulate the unstructured uncertainty inherently associated with any model for the system's RUL. For example, a variation of the fault growth rate may represent the effect of an unexpected change in the environmental conditions of the system, such as the ingress of contaminants in a mechanical transmission.

C. Assessment function

The assessment function relies on a model-based strategy to evaluate the performance of the system under the effect of faults, in order to determine if the current health condition is still compatible with safe system operations. In particular, the specific assessment function employed here evaluates the several features of the system response (including no-load speed, stall load, frequency response, and stability margins). These features are then compared with the applicable performance requirements, in order to determine whether or not they are still met. The assessment function is employed as a stopping criterion in the numerical integration of the damage propagation model. Since the associated computational burden is high, the assessment function is replaced with an SVM surrogate for real-time evaluations, as described in Section II.C.1. Further details on the Assessment Function and a parametric study to optimize the SVM may be found in [49].

IV. Results and Discussion

To demonstrate our original strategy for the real-time reliability assessment of the electromechanical actuator discussed in Section III, we collect two reference dataset – a training dataset and a validation dataset – through the evaluation of the virtual models (Sections III.A, III.B and III.C) for a variety of fault conditions. The training dataset comprises 10000 combinations of fault modes $\boldsymbol{k}$ determined with a particular importance sampling strategy that increases the density of data points near the nominal condition and allows to characterize the effects of small, incipient faults [5]. For each fault combination of the training set, the dynamical model of the actuator (Section III.A) and the Assessment Function (Section III.C) are evaluated. The validation set includes 50 test cases determined with the same sampling technique used for the training set. The two dataset sample the same space of fault modes, but do not share any specific combination of faults $\boldsymbol{k}$. For each test case of the validation set, the damage propagation model III.B is integrated numerically to simulate the evolution of faults to a complete failure. At each integration timestep, the dynamical model of the actuator and the Assessment Function (Section III.C) are evaluated to determine respectively the response of the system (needed as input for the FDI algorithm) and the compliance of that response to the applicable requirements.

Online, the proposed methodology processes the actuator dynamical response through the compression and FDI

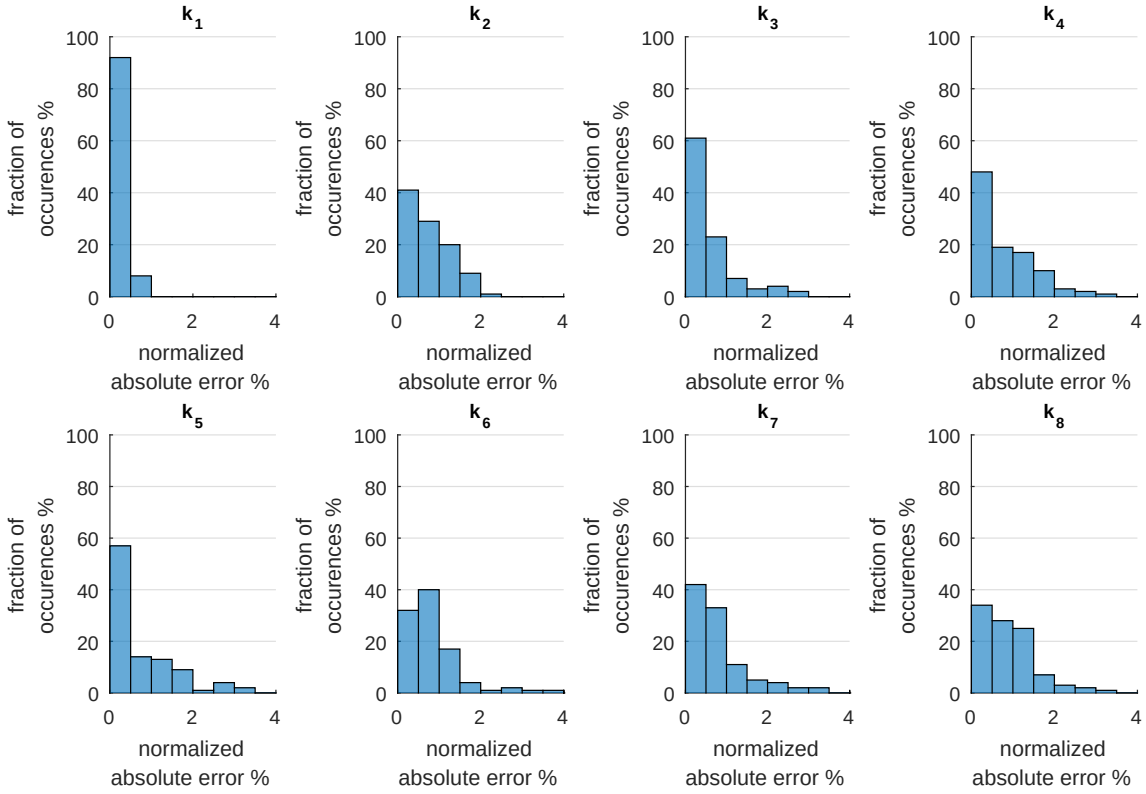

Fig. 6 Distribution of the error associated to FDI, for each fault parameter k_i

steps described in Sections II.A.2 and II.B.2, respectively. The estimate of the system health $\boldsymbol{k}$ is obtained as a result. Figure 6 illustrates the uncertainty distributions associated with these estimates of fault conditions $\boldsymbol{k}$: the histograms shows the modulus of the normalized error e_{na}:

$$e_{na} = \frac{|k^E - k^A|}{\max k^A - \min k^A} \tag{14}$$

where k^E is the estimated fault parameter and k^A is the actual one. The friction fault mode, encoded in the parameter k_1, is captured with better accuracy than the other fault modes. Larger errors are recorded for backlash, eccentricity and gain drift. The partial short circuits are characterized by moderate uncertainty. This behavior mirrors the sensitivity of the specific monitored signal (the stator current of the motor) to each fault mode.

Figure 7 shows the evolution of the RUL estimate when the damage propagation model is constant in time, that is $d\mathrm{A}(t)/dt = 0 \quad \forall t$, where A is the state matrix describing the evolution of faults. At the beginning, the algorithm overestimates the system RUL: indeed, the state and control matrices of Equation 5 are initialized to zero, and the estimated RUL is infinite. The early estimates have a very large dispersion, as both the model of damage propagation and the measurement of the initial condition are affected by uncertainty. The model of damage propagation superimposes a normally distributed noise to the otherwise exponential rate of fault growth; this behavior is clearly visible in Figure 5 and simulates the effect of manufacturing defect and variability of operating conditions experienced by the equipment. Additionally, uncertainty on FDI arises from two sources: the additive white noise acting on the output of the dynamical model of the EMA (simulating the error in measurements) and the error associated to the evaluation of the MLP model. The assimilation of additional observations of the fault propagation history allows to filter out errors inevitably affecting FDI, and to obtain less disperse and more robust predictions of the system life. As time runs, approaching to the right of Figure 7, the estimate of the remaining useful life improves in accuracy thanks to the efficient assimilation from real-time measurements. At first, only a rough value is available, but the expected failure is still far ahead, and a precise information is not needed yet. As the failure approaches, the estimate becomes more accurate, when it is required to plan corrective actions.

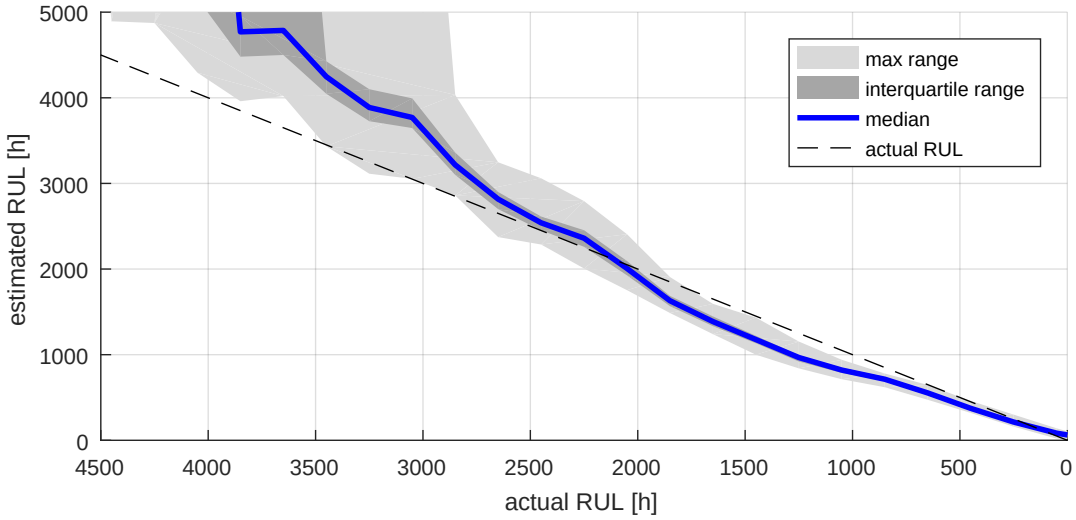

Fig. 7 Comparison between actual and estimated RUL, with a time-invariant damage propagation model. The RUL is estimated every 200 hours, considering the FDI observations of the last 200 operating hours.

Figure 8 shows the evolution of the RUL estimate for a test case where the damage propagates at a variable (increasing) rate, that is $d\mathrm{A}(t)/dt > 0 \quad \exists t$. At the beginning, the actual RUL of the system is overestimated, since the current damage propagation rate is predicted to the complete failure. At $RUL \approx 1800h$, the fault growth rate rises: this event may simulate either an uncertainty in the model (e.g. a given component starts wearing faster after a critical threshold is reached, such as a hardened external layer is completely worn out) or an unpredictable change in the external conditions that affects the wear rate (such as, the lubricant of a sealed transmission may get contaminated and lose its properties). The RUL estimation algorithm reacts to this change by adapting its prediction to the new observed time history of health conditions. As shown in the second part of Figure 8, shortly after the change in damage growth rate the dispersion on the estimation shrinks and the median RUL estimate moves closer to the actual one.

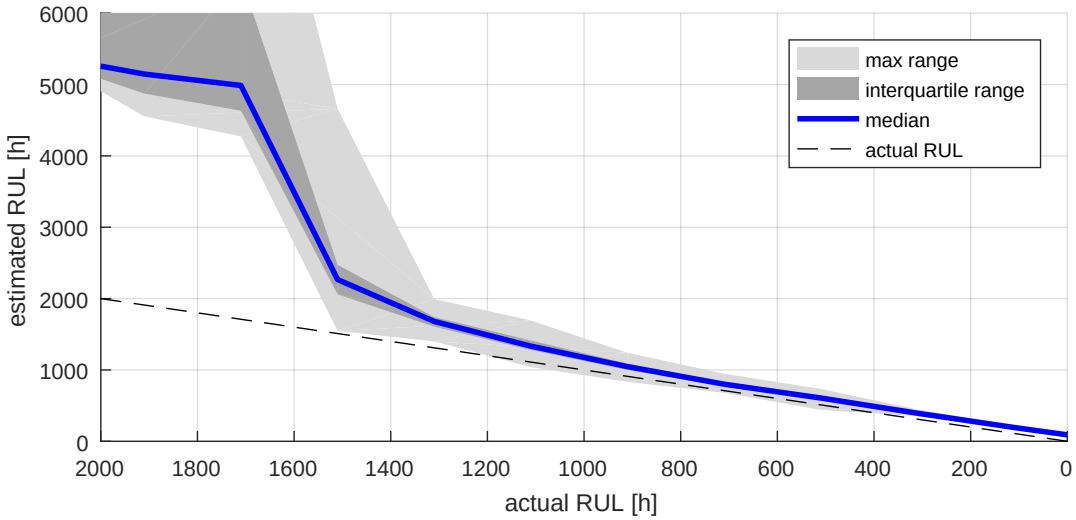

Fig. 8 Comparison between actual and estimated RUL with a time-varying model. The reference damage propagation rate increases at $RUL \approx 1800h$

Table 1 summarizes the error associated with the RUL prediction in the two test cases of Figures 7 and 8. The early estimates are characterized by a large uncertainty, particularly in the case of a time-varying damage growth rate. As the actual RUL decreases, the algorithm is able to get the prediction within ±20% of the exact value. This error is coherent with most approaches available in literature, and is mainly due to the inherent variability associated to the fault growth. The advantage introduced with our approach is that we efficiently learn in real-time to compute predictions of the Remaining Useful Life. The whole online process runs in the Matlab environment, on a laptop PC with an i7-6500U processor and 8GB of memory. The computational time required for each FDI and RUL estimate ranges between 0.1s and 1s, which makes it suitable for on-board, nearly real-time execution.

Table 1 Median relative error in RUL prediction

actual RUL, h	error - time-invariant fault growth	error - time-varying fault growth
3000	23,90%	243,64%
1500	-18,85%	50,11%
500	-17,04%	18,95%

V. Conclusions

A novel method for the estimation of Remaining Useful Life of aerospace systems and on-board equipment has been developed. The strategy processes and assimilates the available observations of the system health condition to infer a model of damage propagation and estimate the remaining time to failure; no prior knowledge of the wear rate of the involved components is required. The proposed methodology achieves an accuracy comparable to similar approaches available in literature, since the limiting factor tends to be the variability in fault propagation rate that is inherent to dynamical system. However, the strength of the proposed method lies in its ability to deal with unstructured uncertainties and to adapt to unexpected variations in the fault propagation dynamics. This way, an acceptable accuracy in RUL prediction is kept even when an unexpected event modifies the wear rate of the components, or when fault detection is affected by a large uncertainty.

Our strategy dynamically assimilates new information from the observed time-evolution of the health condition of the system and updates a model of damage propagation to yield an accurate estimate of the RUL, acknowledging the effect of any changes in the operating condition of the equipment. The entire RUL estimation process requires limited computational resources, and can be performed in real-time to inform the planning of maintenance interventions and ensure the safety of operations. This will ease the early and safe integration of innovative technology in aerospace systems. Future developments will include a better characterization of the uncertainty associated with the RUL estimate and the validation of the EMA models in faulty conditions.

Acknowledgments

The authors wish to thank Prof. Paolo Maggiore for his support. This work was funded by the Visiting Professor grant awarded to Dr. Ing. Laura Mainini under the Visiting Professor program of Politecnico di Torino, and by the Ph.D. grant awarded to Pier Carlo Berri at Politecnico di Torino.

References

[1] Vachtsevanos, G., Lewis, F., Roemer, M., Hess, A., and Wu, B., *Intelligent Fault Diagnosis and Prognosis for Engineering Systems*, John Wiley & Sons, Inc., 2006.

[2] Quigley, R., "More Electric Aircraft," *Proceedings Eighth Annual IEEE Applied Power Electronics Conference and Exposition*, IEEE, San Diego, CA, 7-11 March 1993.

[3] Howse, M., "All-electric aircraft," *Power Engineer*, Vol. 17, No. 4, 2003, p. 35.

[4] Berri, P. C., Dalla Vedova, M. D. L., and Mainini, L., "Diagnositcs of actuation systems faults from dynamic data," *6th European Conference on Computational Mechanics (ECCM)*, Glasgow, UK, 11-15 June 2018.

[5] Berri, P. C., Dalla Vedova, M. D. L., and Mainini, L., "Real-time Fault Detection and Prognostics for Aircraft Actuation Systems," *2019 AIAA SciTech Forum*, American Institute of Aeronautics and Astronautics, (AIAA Paper 2019-2210), AIAA, San Diego, California, 2019.

[6] Schmitz, T., "Wear-Rate Uncertainty Analysis," *Transactions of the ASME - Journal of Tribology*, Vol. 126, 2004, pp. 802–808.

[7] Burris, D. L., and Sawyer, W. G., "Measurement Uncertainties in Wear Rates," *Tribology Letters*, Vol. 36, No. 01, 2009, pp. 81–87. https://doi.org/10.1007/s11249-009-9477-8.

[8] Wu, X., and Balakrishnan, N., "Variance-based importance analysis measure for mission reliability of phased mission system," *Journal of Statistical Computation and Simulation*, Vol. 88, 2017, pp. 1–28. https://doi.org/10.1080/00949655.2017.1407936.

[9] Okoh, C., Roy, R., Mehnen, J., and Redding, L., "Overview of Remaining Useful Life Prediction Techniques in Through-life Engineering Services," *Procedia CIRP*, Vol. 16, 2014, pp. 158 – 163. https://doi.org/https://doi.org/10.1016/j.procir.2014.02.006, product Services Systems and Value Creation. Proceedings of the 6th CIRP Conference on Industrial Product-Service Systems.

[10] Karandikar, J., Abbas, A., and Schmitz, T., "Remaining useful tool life predictions in turning using Bayesian inference," *International Journal of Prognostics and Health Management*, Vol. 4, 2013.

[11] Grosso, L., De Martin, A., Jacazio, G., and Sorli, M., "Development of data-driven PHM solutions for robot hemming in automotive production lines," *International Journal of Prognostics and Health Management*, Vol. 11, 2020.

[12] Orrell, D., "Filtering chaos: a technique to estimate dynamical and observational noise in nonlinear systems," *International Journal of Bifurcation and Chaos*, Vol. 15, No. 01, 2005, pp. 99–107. https://doi.org/10.1142/S021812740501203X.

[13] Rahimi Mousavi, M. S., and Boulet, B., "Dynamical modeling and optimal state estimation using Kalman-Bucy filter for a seamless two-speed transmission for electric vehicles," *2015 23rd Mediterranean Conference on Control and Automation (MED)*, 2015, pp. 76–81. https://doi.org/10.1109/MED.2015.7158732.

[14] Nesci, A., De Martin, A., Jacazio, G., and Sorli, M., "Detection and Prognosis of Propagating Faults in Flight Control Actuators for Helicopters," *MDPI Aerospace*, Vol. 7, No. 3, 2020, p. 20. https://doi.org/https://doi.org/10.3390/aerospace7030020.

[15] Tinga, T., and Loendersloot, R., *Physical Model-Based Prognostics and Health Monitoring to Enable Predictive Maintenance*, Springer, 2019, pp. 313–353. https://doi.org/10.1007/978-3-030-05645-2_11.

[16] Engelberth, T., Krawczyk, D., and Verl, A., "Model-based method for condition monitoring and diagnosis of compressors," *Procedia CIRP*, Vol. 72, 2018, pp. 1321 – 1326. https://doi.org/https://doi.org/10.1016/j.procir.2018.03.271, 51st CIRP Conference on Manufacturing Systems.

[17] Huang, B., Di, Y., Jin, C., and Lee, J., "Review of data-driven prognostics and health management techniques: lessions learned from PHM data challenge competitions," 2017.

[18] Qian, P., Ma, X., Zhang, D., and Wang, J., "Data-Driven Condition Monitoring Approaches to Improving Power Output of Wind Turbines," *IEEE Transactions on Industrial Electronics*, Vol. 66, No. 8, 2019, pp. 6012–6020.

[19] Frank, S., Heaney, M., Jin, X., Robertson, J., Cheung, H., Elmore, R., and Henze, G., "Hybrid Model-Based and Data-Driven Fault Detection and Diagnostics for Commercial Buildings," *2016 ACEEE Summer Study on Energy Efficiency in Buildings*, Pacific Grove, California, 2016.

[20] Slimani, A., Ribot, P., Chanthery, E., and Rachedi, N., "Fusion of Model-based and Data-based Fault Diagnosis Approaches," *IFAC-PapersOnLine*, Vol. 51, No. 24, 2018, pp. 1205–1211.

[21] Sidhu, A., Izadian, A., and Anwar, S., "Adaptive Nonlinear Model-Based Fault Diagnosis of Li-Ion Batteries," *IEEE Transactions on Industrial Electronics*, Vol. 62, No. 2, 2015, pp. 1002–1011. https://doi.org/10.1109/TIE.2014.2336599.

[22] Kim, K., and Parlos, A. G., "Model-based fault diagnosis of induction motors using non-stationary signal segmentation," *Mechanical Systems and Signal Processing*, Vol. 16, No. 2, 2002, pp. 223–253. https://doi.org/10.1006/mssp.2002.1481.

[23] Qin, S. J., "Data-driven Fault Detection and Diagnosis for Complex Industrial Processes," *IFAC Proceedings Volumes*, Vol. 42, No. 8, 2009, pp. 1115 – 1125. https://doi.org/10.3182/20090630-4-ES-2003.00184, 7th IFAC Symposium on Fault Detection, Supervision and Safety of Technical Processes.

[24] Sarkar, S., Jin, X., and Ray, A., "Data-Driven Fault Detection in Aircraft Engines With Noisy Sensor Measurements," *Journal of Engineering for Gas Turbines and Power*, Vol. 133, 2011, pp. 081602–1. https://doi.org/10.1115/1.4002877.

[25] Sirovich, L., "Turbulence and the dynamics of coherent structures. Part 1: Coherent structures," *Quarterly of Applied Mathematics*, Vol. 45, No. 3, 1987, pp. 561–571.

[26] Hinze, M., and Volkwein, S., "Proper Orthogonal Decomposition Surrogate Models for Nonlinear Dynamical Systems: Error Estimates and Suboptimal Control," *Lecture Notes in Computational Science and Engineering*, Springer-Verlag, 2005, pp. 261–306.

[27] Candès, E. J., Romberg, J. K., and Tao, T., "Stable signal recovery from incomplete and inaccurate measurements," *Communications on Pure and Applied Mathematics*, Vol. 59, No. 8, 2006, pp. 1207–1223.

[28] Kunisch, K., and Volkwein, S., "Control of the Burgers Equation by a Reduced-Order Approach Using Proper Orthogonal Decomposition," *Journal of Optimization Theory and Applications*, Vol. 102, No. 2, 1999, pp. 345–371.

[29] Kohonen, T. (ed.), *Self-organizing Maps*, 3rd ed., Springer-Verlag, Berlin, Heidelberg, 2001.

[30] Tarek, A., Yassine, K., and Toumi, A., "Clustering of the Self-Organizing Map based Approach in Induction Machine Rotor Faults Diagnostics," *Leonardo Journal of Sciences*, Vol. 15, 2009.

[31] Svensson, M., Byttner, S., and Rognvaldsson, T., "Self-organizing maps for automatic fault detection in a vehicle cooling system," *2008 4th International IEEE Conference Intelligent Systems*, Vol. 3, 2008, pp. 24–8–24–12. https://doi.org/10.1109/IS.2008.4670481.

[32] Mainini, L., and Willcox, K. E., "Sensor placement strategy to inform decisions," *18th AIAA/ISSMO Multidisciplinary Analysis and Optimization Conference*, AIAA Aviation Forum, (AIAA Paper 2017-3820), AIAA, Denver, Colorado, 5-9 June 2017.

[33] Mainini, L., "Structural assessment and sensor placement strategy for self-aware aerospace vehicles," *Structural Health Monitoring 2017: Real-Time Material State Awareness and Data-Driven Safety Assurance*, Vol. 1, 2017, pp. 1586–1594.

[34] Everson, R., and Sirovich, L., "Karhunen–Loève procedure for gappy data," *Journal of the Optical Society of America A*, Vol. 12, No. 8, 1995, p. 1657.

[35] Bishop, C. M., *Pattern Recognition and Machine Learning (Information Science and Statistics)*, Springer-Verlag, Berlin, Heidelberg, 2006.

[36] Hagan, M., and Menhaj, M., "Training feedforward networks with the Marquardt algorithm," *IEEE Transactions on Neural Networks*, Vol. 5, No. 6, 1994, pp. 989–993.

[37] E. Fahlman, S., "An Empirical Study of Learning Speed in Back-Propagation Networks," *Technical Report CMU-CS-88-162, CMU*, 1999.

[38] Huston, D., *Structural sensing, health monitoring, and performance evalaution*, CRC Press, 2011.

[39] Cortes, C., and Vapnik, V., "Support-Vector Networks," *Machine Learning*, Vol. 20, No. 3, 1995, pp. 273–297.

[40] Gestel, T. V., Suykens, J. A. K., Baesens, B., Viaene, S., Vanthienen, J., Dedene, G., Moor, B. D., and Vandewalle, J., "Benchmarking Least Squares Support Vector Machine Classifiers," *Machine Learning*, Vol. 54, 2004, pp. 5–32.

[41] Basudhar, A., and Missoum, S., "Adaptive explicit decision functions for probabilistic design and optimization using support vector machines," *Computers & Structures*, Vol. 86, No. 19, 2008, pp. 1904 – 1917. https://doi.org/https://doi.org/10.1016/j.compstruc.2008.02.008, URL http://www.sciencedirect.com/science/article/pii/S0045794908000515.

[42] Leng, Q., Wang, S., and Shen, D., "Construction of Binary Tree Classifier Using Linear SVM for Large-Scale Classification," *2018 International Conference on Robots & Intelligent System (ICRIS)*, IEEE, Changsha, China, 26-27 May 2018.

[43] Mornacchi, A., Vachtsevanos, G., and Jacazio, G., "Prognostics and Health Management of an Electro-Hydraulic Servo Actuator," *Annual Conference of the Prognostics and Health Management Society*, San Diego, CA, USA, 19-24 October 2015.

[44] Berri, P. C., Dalla Vedova, M. D., and Maggiore, P., "A Lumped Parameter High Fidelity EMA Model for Model-Based Prognostics," *Proceedings of the 29th European Safety and Reliability Conference*, 2019. https://doi.org/10.3850/978-981-11-2724-3_0480-cd.

[45] Berri, P. C., Dalla Vedova, M. D., Maggiore, P., and Viglione, F., "A simplified monitoring model for PMSM servoactuator prognostics," *9th EASN International Conference on "Innovation in Aviation & Space"*, 2019. https://doi.org/10.1051/matecconf/201930404013.

[46] Stevens, B. L., and Lewis, F. L., *Aircraft Control and Simulation*, John Wiley & sons, inc., 1992.

[47] Sciandra, P., "Development and experimental validation of prognostic algorithms for electromechanical actuators," Master's thesis, Politecnico di Torino, Turin, Italy, 2020.

[48] Boschetti, V., "Development of an experimental test bench for the validation of prognostic algorithms for electromechanical actuators," Master's thesis, Politecnico di Torino, Turin, Italy, 2020.

[49] Berri, P. C., Dalla Vedova, M. D., Maggiore, P., and Quattrocchi, G., "Model-based strategy and surrogate function for health condition assessment of actuation devices," *10th EASN virtual conference*, 2020 (in press).